Silver Nanocrystals

DOI: 10.1002/ange.200601277

Polyhedral Silver Nanocrystals with Distinct Scattering Signatures**

*Andrea Tao, Prasert Sinsermsuksakul, and Peidong Yang**

Subwavelength silver nanoparticles display a variety of unrivaled optical properties in the visible and near-IR regime, including scattering cross-sections that are orders of magnitude higher than the fluorescence emission from organic dyes as well as intense local amplification of electromagnetic fields. These phenomena result from localized surface plasmons (LSPs), where the plasma oscillations of free electrons in the metal are bound by nanoparticle geometry. Plasmon excitation occurs when a photon is absorbed at a metal–dielectric interface, transferring energy into the collective oscillations of conduction electrons, which are coupled in-phase with incident radiation. For silver and gold nanoparticles, these resonant frequencies occur at wavelengths in the visible region, giving rise to the brilliant colors that are characteristic of their colloidal solutions.

For silver particles with diameter $d \ll \lambda$, a single dipolar plasmon mode is allowed.[1] However, for particles with lower symmetry or anisotropic dielectric surroundings, the nature of

[*] A. Tao, P. Sinsermsuksakul, Prof. P. Yang
Department of Chemistry
University of California, Berkeley
Materials Science Division
Lawrence Berkeley National Laboratory
Berkeley, CA 94720 (USA)
Fax: (+1) 510-642-7301
E-mail: p_yang@berkeley.edu

[**] We thank Tevye Kuykendall and Susan Habas for technical assistance and helpful discussions. This work was supported by the Office of Basic Science, Department of Energy. A.R.T. gratefully acknowledges the National Science Foundation for a graduate research fellowship. We thank the National Center for Electron Microscopy for the use of their facilities.

Supporting information for this article is available on the WWW under http://www.angewandte.org or from the author.

these LSP modes is more difficult to map. Elongated shapes such as nanowires and rods experience a "lightning-rod effect", whereby the metal structure acts as an antenna for electromagnetic field amplification as a result of highly polarized LSPs.[2] Nanostructures that contain sharp vertexes, such as triangular plates[3] and icosahedra,[4] have also been shown to exhibit multipolar plasmon modes. Principally, polyhedral shapes with well-defined facets and corners are predicted to have distinct scattering signatures in addition to scattering efficiencies that are orders of magnitude higher than those of their spherical counterparts.[5] Scanning near-field[6] and TEM-correlated darkfield experiments[7] are among the few experimental attempts to spatially resolve these shape-dependent plasmons. Here, we employ a strategic synthetic approach to correlate nanocrystal geometry with specific LSP modes, investigating the systematic shape evolution of polyhedral nanocrystals.

We synthesized monodisperse colloidal solutions of silver nanocrystals with regular polyhedral shapes and bound entirely by {100} and {111} facets of the fcc crystal lattice (Figure 1 a). These nanocrystals were synthesized using the polyol method,[8] where the metal salt is reduced by a diol solvent at near-reflux temperatures ($\approx 180\,^{\circ}C$) in the presence of a polymeric stabilizing agent. We used poly(vinyl pyrrolidone) (PVP) as the capping polymer as it has been demonstrated to be a successful shape control agent for fcc metals.[9,10] We adapted the synthetic procedure first developed by Sun and Xia,[9] who reported the use of PVP for the formation of silver nanocubes. In a typical synthesis, silver nitrate and PVP were dissolved separately and then injected periodically into a solution of hot pentanediol. Depending on how long these sequential additions are continued, specific polyhedral shapes can be obtained in high yield.

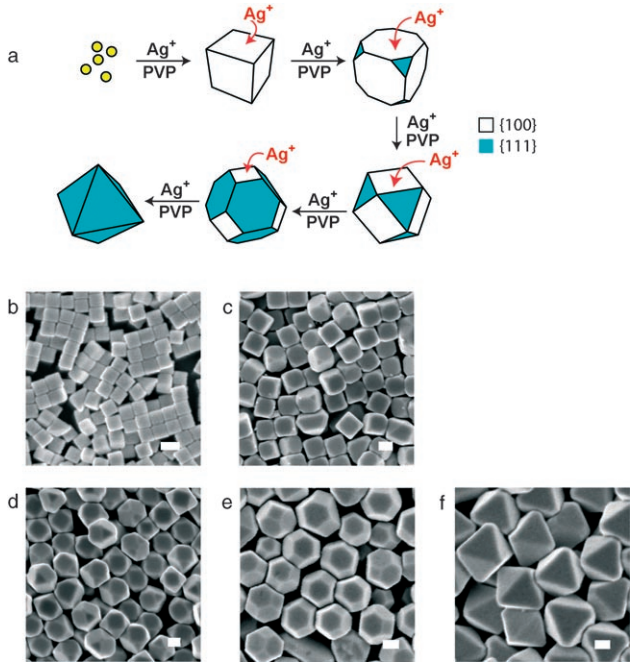

Figure 1. By extending the polyol reaction for a given time period, various polyhedral shapes capped with {100} and {111} faces can be obtained in high yield. a) A schematic of the nucleation and growth process, in which silver continuously deposits onto the {100} facet to eventually result in a completely {111}-bound octahedron. b–f) SEM images of cubes, truncated cubes, cuboctahedra, truncated octahedra, and octahedra, respectively (scale bar: 100 nm).

As seen in the scanning electron microscopy (SEM) images in Figure 1 b–f, we synthesized a variety of nanocrystal shapes with uniform sizes: cubes ($d \approx 80$ nm), truncated cubes ($d \approx 120$ nm), cuboctahedra ($d \approx 150$–200 nm), truncated octahedra ($d \approx 200$–250 nm), and octahedra ($d \approx 250$–300 nm). Transmission electron microscopy images (see Supporting Information) confirm that the polyhedra are single-crystalline and exhibit atomically defined facets with sharp edges and corners. Although similar truncated shapes have been previously observed,[11] this is the first observation of metallic octahedral nanocrystals as the majority product. On the basis of energetic considerations, the optimal particle shape for an fcc metal is a truncated octahedron with regular hexagonal faces.[12] Thus, the formation of octahedra suggests that the polyhedral nanocrystals observed here result from a kinetically limited reaction equilibrium.

To investigate this growth mechanism, we employed UV/Vis absorption spectrometry (Agilent, UV/Visible Chemstation) to probe shape-specific LSPs in the optical frequencies. Figure 2 displays a plot of the dipolar plasmon wavelength as a function of reaction time. This LSP mode is associated with nanoparticle volume and undergoes a red shift with increasing diameter. The graph indicates that shape evolution occurs in two steps: fast nucleation, which occurs at an exponential rate, and slow growth, which occurs at a linear rate. Initially, small silver particles (< 10 nm) nucleate and develop into nanocubes bound by {100} planes, which are thought to be selectively stabilized by adsorbed PVP. As the reaction is continued, silver deposits selectively onto the {100} nanocrystal facets rather than growing in a layer-by-layer fashion (Figure 1 a). The {111}-capped corners of the nanocube are stabilized during this growth period in which the nanocrystal evolves from a {100}-bound cube to a {111}-bound octahedron. The stability of both {100} and {111} planes in the presence of PVP indicates that shape control may not be

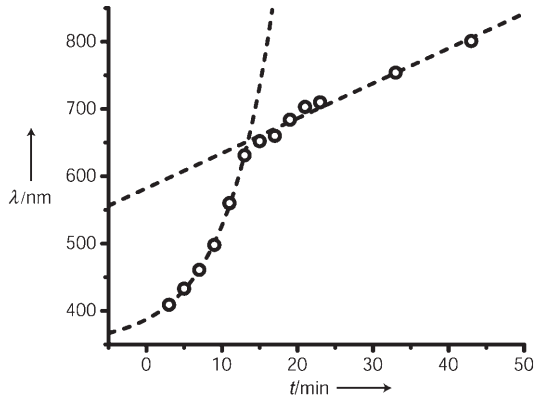

Figure 2. Plot of reaction time versus dipolar surface plasmon wavelength, which is correlated to nanocrystal volume. Exponential nanocrystal growth corresponds to the nucleation process, whereas the linear regime corresponds to slow layer-by-layer growth.

explicitly dictated by the capping polymer. Rather, preferential crystal growth seems to result from a kinetically limited equilibrium influenced heavily by reaction parameters such as temperature, reactant concentration, and reactant molar ratios.

UV/Vis spectra were obtained after the colloidal solutions were repeatedly washed with ethanol to remove excess polymer and filtered (Millipore, DVPP Durapore Membrane Filters). The extinction spectra (extinction = scattering + absorption) in Figure 3a show the differences in LSP modes for colloidal suspensions of cubes, cuboctahedra, and octahedra, all of which exhibit highly complex plasmon signatures as a result of their geometric anisotropy. These LSPs can be assigned by comparing experimental extinction spectra with theoretical extinction cross-section curves calculated using the discrete dipole approximation (DDA).[13] DDA is an analytical method used to model light scattering by small particles, whose optical properties experience strong variation with particle size, shape, and local environment. We used an algorithm developed by Draine and Flatau[14] in which the nanocrystal is represented by a scattering target composed of point dipoles and is subjected to an incident plane wave. As seen in Figure 3b,c, the theoretical curves obtained with this method agree remarkably well with our experimental data. Note that because DDA calculations were performed for a vacuum environment, the experimental resonances appear slightly red-shifted (< 10 nm) as expected for a higher dielectric medium.

With this data, we can begin to relate optical signature with the physical geometry of each silver nanocrystal shape. The optical properties of silver nanocubes with an edge length $a = 30$ nm have been studied in depth in Reference [15] with respect to different refractive media, but only two resonances were observed for these particles. For nanocubes with $a =$ 80 nm, the theoretical curve predicts six strong LSP resonances. The lowest frequency (first and second) modes at $\lambda \approx 480$ nm and $\lambda \approx 550$ nm correspond to quadrupolar and dipolar LSP modes, respectively. The quadrupolar mode is the sharpest and the strongest LSP mode. For truncated cubes whose corners are replaced by a flat {111} facet, this LSP mode disappears (see Supporting Information). This indicates that for the quadrupolar mode, amplitude is particularly high at the eight corners of the cube. As the cube truncates and develops increasingly larger {111} facets, the third and fourth plasmon modes increasingly dominate the scattering spectrum. For a cuboctahedron with $a = 151$ nm, these modes are red-shifted and appear at $\lambda \approx 430$ nm and $\lambda \approx 480$ nm. Thus, for the third and fourth LSP modes, amplitude is strongly associated with the edges of the polyhedra. Previous calculations in which the optical absorption of NaCl crystals was predicted qualitatively agree with these spatial assignments.[16]

The characteristic optical signature for octahedral-shaped nanocrystals is much greater in complexity compared to the other polyhedral shapes, despite their shared O_h symmetry. Octahedral particles exhibit several strong LSP modes as well as fine structure in the form of many less-intense resonances (Figure 3a). This fine structure is well-resolved in the UV/Vis spectrum in the 400–600 nm range, where no less than six LSP bands can be clearly distinguished. DDA calculations (Figure 3b) assign these higher frequency LSPs as hexapolar and higher-order modes, while the resonances at $\lambda \approx 800$ nm are mainly quadrupolar in nature.

Extinction measurements for colloidal solutions, however, are bulk measurements which rely on sample homogeneity. To investigate shape-

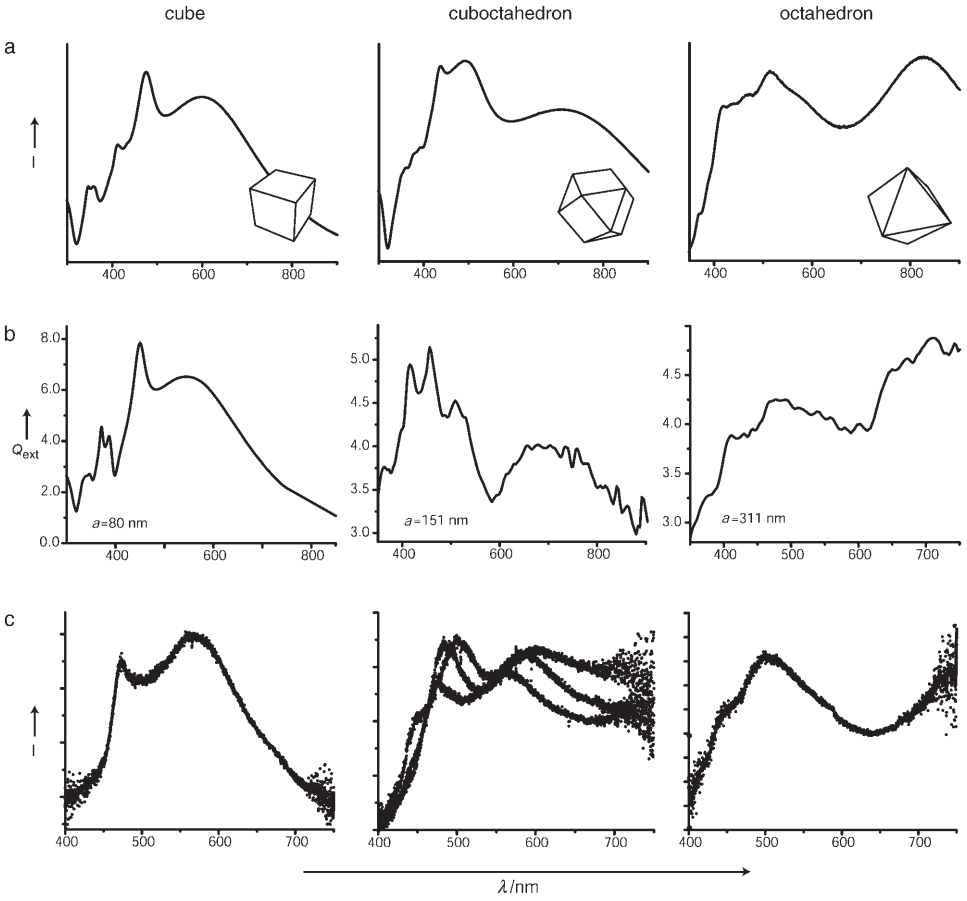

Figure 3. Silver nanocubes, cuboctahedra, and octahedra display distinct scattering signatures despite possessing the same point group symmetry. a) UV/Vis spectra of colloidal dispersions. b) DDA simulations for single particles of each shape, where *a* is the edge length for the polyhedron. c) Darkfield scattering spectra for single nanocrystals. For cuboctahedra, varying degrees of truncation exist within the sample.

dependent scattering at the single-particle level, we also collected darkfield Rayleigh scattering signals from individual nanocrystals. In these experiments, a drop of the colloidal solution was cast onto a glass coverslip and irradiated with a tungsten lamp. The scattering colors of the silver nanocrystals were observed by using an inverted microscope (Olympus IX71) equipped with a darkfield condenser and collection objective. The images in Figure 4 are real colors captured by a digital camera (Olympus DP70, 12MP). Each colored circle is the total scattered light from a single nanocrystal. Cubes ($a \approx 80$ nm) strongly scatter green light, given that their strongest LSP resonances occur around $\lambda \approx 500$–550 nm. As the nanocrystal shape increases in volume and evolves into its truncated forms, the scattering color changes from green to yellow and eventually to the red-orange color characteristic of octahedra ($a \approx 300$ nm).

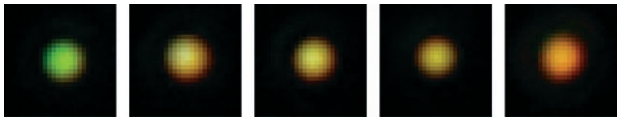

Figure 4. Real color images taken with a digital camera displaying the different colors that result from plasmon-mediated scattering. Each spot corresponds to the light scattered from a single nanocrystal. From left to right: cube, truncated cube, cuboctahedron, truncated octahedron, and octahedron. The color evolves from green to orange with increasing degrees of truncation.

Scattering spectra from single nanocrystals can be obtained by directing scattered light to an imaging CCD and spectrometer. The sample preparation is identical to the aforementioned experiments, in which the nanocrystals are cast onto a glass substrate. This sampling geometry, however, is conducive to substrate effects because the particle is in intimate contact with two different media: glass and air. This anisotropic dielectric environment can greatly influence LSPs.[17] To prevent this effect, we prepared our nanocrystals with a thick (≈ 50 nm) silica shell to ensure a homogenous dielectric surrounding (see Supporting Information). In general, increasing the refractive index of the nanocrystal environment leads to a red shift in the frequencies of allowed plasmon modes but the overall line shape is unaffected, which can be confirmed experimentally by UV/Vis measurements. Figure 3c shows representative scattering signatures for single nanocrystals with cubic, cuboctahedral, and octahedral shapes. Although only the most intense LSP bands appear, the spectra for the cube and octahedron agree well with UV/Vis extinction measurements (absorption effects are negligible above 400 nm) and DDA calculations. Three representative scattering spectra for cuboctahedral nanocrystals are shown in Figure 3c because varying degrees of truncation exist within the same sample. It is perhaps this shape variance that accounts for the lack of fine structure predicted by theory and a broadening of LSP peaks in the UV/Vis spectrum of the colloidal solution.

Thus far, we have investigated LSPs for different polyhedral nanocrystals for both isotropically distributed colloidal suspensions and isolated single particles. From both a theoretical and experimental standpoint, the nature of these modes is of great interest given their ability to spatially confine light to a metal–dielectric interface. The ability to engineer metallic nanocrystals that allow the excitation of specific localized surface plasmon modes should have profound consequences for research fields such as surface-enhanced Raman spectroscopy[18,19] or plasmonic transport.[20] Future experiments may further elucidate the mechanism for local field amplification and electromagnetic coupling, in addition to providing important optical characterization of these metallic nanoscale building blocks.

Experimental Section

Nanocrystal synthesis: Silver nitrate (0.50 g) and copper(II) chloride (0.86 μg) were dissolved in 1,5-pentanediol (12.5 mL) in a glass vial. In a separate vial, PVP ($M_w = 55\,000$ amu, 0.25 g) was dissolved in 1,5-pentanediol (12.5 mL). Using a temperature-controlled silicone oil bath, 1,5-pentanediol (20 mL) was heated for 10 min. The two precursor solutions were then injected into the hot reaction flask at different rates: 500 μL of the silver nitrate solution every minute and 250 μL of the PVP solution every 30 s. For nanocubes, this addition was stopped once the solution turned opaque (≈ 6 min). For truncated cubes, cuboctahedra, and octahedra, the addition of precursor solutions was continued for a longer period of time ($\approx$120 min for octahedral nanocrystals).

Silica coating: 5 mL of colloidal solution was diluted with propan-2-ol (15 mL) and deionized water (5 mL). While stirring vigorously, tetraethoxysilane (400 μL) and ammonium hydroxide (400 μL) were added to the mixture. The reaction was allowed to proceed for 10 min before the solution was centrifuged and the precipitate was collected.

Darkfield scattering measurements: A dilute colloidal solution of nanocrystals was drop-cast onto a clean glass coverslip and then dried under vacuum ($\approx 10^{-2}$ Torr). Samples were then illuminated with a 100-W halogen bulb using a darkfield condenser (NA = 1.2–1.4) with immersion oil. Light was collected through a 60× microscope objective lens (NA = 0.7) and captured by a 1340 × 400-pixel back-illuminated CCD (Princeton Instruments, Spec-10:400B) and spectrometer (Princeton Instruments, SpectraPro 2300i).

Received: April 1, 2006
Published online: June 22, 2006

Keywords: colloids · nanostructures · silver · surface plasmon resonance

[1] C. F. Bohren, D. R. Huffman, *Absorption and Light Scattering of Light by Small Particles*, Wiley-Interscience, New York, **1983**.
[2] C. Sonnichsen, T. Franzl, T. Wilk, G. von Plessen, J. Feldmann, O. Wilson, P. Mulvaney, *Phys. Rev. Lett.* **2002**, *88*, 077402/1.
[3] J. E. Millstone, S. Park, K. L. Shuford, L. Qin, G. C. Schatz, C. A. Mirkin, *J. Am. Chem. Soc.* **2005**, *127*, 5312.
[4] A. S. Kumbhar, M. K. Kinnan, G. Chumanov, *J. Am. Chem. Soc.* **2005**, *127*, 12444.
[5] I. O. Sosa, C. Noguez, R. G. Barrera, *J. Phys. Chem. B* **2003**, *107*, 6269.
[6] S. Kawata, *Top. Appl. Phys.* **2001**, *81*, 1.
[7] J. J. Mock, M. Barbic, D. R. Smith, D. A. Schultz, S. Schultz, *J. Chem. Phys.* **2002**, *116*, 6755.
[8] F. Fievet, J. P. Lagier, B. Blin, B. Beaudoin, M. Figlarz, *Solid State Ionics* **1989**, 198.
[9] Y. Sun, Y. Xia, *Science* **2002**, *298*, 2176.

[10] F. Kim, S. Connor, H. Song, T. Kuykendall, P. Yang, *Angew. Chem.* **2004**, *116*, 3759–3763; *Angew. Chem. Int. Ed.* **2004**, *43*, 3673.
[11] B. Wiley, T. Herricks, Y. Sun, Y. Xia, *Nano Lett.* **2004**, *4*, 1733.
[12] J. W. M. Frenken, P. Stoltze, *Phys. Rev. Lett.* **1999**, *82*, 3500.
[13] E. M. Purcell, C. R. Pennypacker, *Astrophys. J.* **1973**, *361*, 705.
[14] B. T. Draine, P. J. Flatau, *J. Opt. Soc. Am.* **1994**, *A11*, 1491.
[15] L. J. Sherry, S.-H. Chang, B. J. Wiley, Y. Xia, G. C. Schatz, R. P. Van Duyne, *Nano Lett.* **2005**, *5*, 2034.
[16] R. Fuchs, *Phys. Rev. B* **1975**, *11*, 1732.
[17] K. L. Kelly, E. Coronado, L. L. Zhao, G. C. Schatz, *J. Phys. Chem. B* **2003**, *107*, 668.
[18] R. G. Freeman, K. C. Grabar, K. J. Allison, R. M. Bright, J. A. Davis, A. P. Guthrie, M. B. Hommer, M. A. Jackson, P. C. Smith, D. G. Walter, M. J. Natan, *Science* **1995**, *267*, 1629.
[19] M. Moskovits, *Rev. Mod. Phys.* **1985**, *57*, 783.
[20] W. L. Barnes, A. Dereux, T. W. Ebbesen, *Nature* **2003**, *424*, 824.

